

Modelling urban stormwater drainage overflows for assessing flood hazards: Application to the urban area of Dakar (Senegal)

Laurent Pascal Malang Diémé^{1, 2}, Christophe Bouvier², Ansoumana Bodian¹ and Alpha Sidibé³

¹ Laboratoire Leïdi “Dynamique des Territoires et Développement”, Université Gaston Berger (UGB), Saint Louis, Sénégal

5 ² IRD, UMR 5151, HSM, Univ. Montpellier, CNRS, IRD, Montpellier, France

³DPGI “Direction de la Prévention et de la Gestion des Inondations au Sénégal”, MEA, Sénégal

Correspondence to: Laurent P. M. Diémé (dieme.laurent-pascal-malang@ugb.edu.sn)

Abstract.

With the recurrence of flooding in African cities, there is growing interest in developing sufficiently informative tools to help characterize and predict overflow risks. One of the challenges is to develop methods that strike a compromise between the accuracy of simulations, the availability of basic data, and the shortening of calculation times to be compatible with real-time applications. The present study carried out on the urban outskirts of Dakar, aims to propose a method capable of modelling flows at fine resolution (25m²), over the entire area, and providing a rapid diagnosis of how the drainage network is operating for rainfall intensities of different return periods while taking urban conditions into account. Three methodological steps are combined to achieve this objective: (i) determination of drainage directions, including modifications induced by buildings, artificial drainage, and storage basins, (ii) application of a hydrological model for calculating flows at the outlets of elementary catchment, (iii) implementation of a hydraulic model for propagating these flows through the drainage network and a storage model for retention basins. The modelling chain was built within the ATHYS platform. The network overflow points are detected if the difference between the calculated flows exceed the network capacity to evacuate them. Examples are given by carrying out simulations using 10 and 100-years design rainfall. . The model also provides boundary conditions for applying more complex hydraulic models to determine the local impact of drainage network overflows on limited areas. However, the goodness of the method still needs to be validated in further research by comparing with accurate data from observed flood events.

1 Introduction

25 African cities are frequently subject to flooding (Yengoh et al., 2017; Tazen et al., 2018; Sy et al., 2020; Barau and Wada, 2021), which results in significant socio-economic, health, and environmental damage (Miller et al., 2022a; Sakijege and Dakyaga, 2023). The current trend toward more intense rainfall (Taylor et al., 2017; Bichet and Diedhiou, 2018; Nkrumah et al., 2019; Klutse et al., 2021), attributed to climate change (Panthou et al, 2018; Chagnaud et al., 2022) and the very rapid dynamics of urbanization (Sène, 2018; Williams et al., 2019; Yuan et al., 2023), are expected to increase the occurrence of

30 urban flooding (Gaisie and Cobbinah, 2023). This is a major source of concern for political decision-makers and city dwellers (Moulds et al., 2021) in these African conurbations, where the gap between adaptation needs and existing tools is wide (Nkwunonwo et al., 2020; Miller, et al., 2022b).

In response to growing adaptation needs (Kreibich et al., 2017; Mashi et al., 2020), interest is being shown in flood characterization (Coulibaly et al., 2020) and forecasting (Chen et al., 2015). The scientific literature reports on several
35 methods implemented, in urban environments, to provide flood assessment and mapping (Henonin et al., 2013; Agonafir et al., 2023). The simplest methods, without introducing simulations of runoff formation, rely on the topographical characteristics of the territory to give a first local estimate of flood risk by the accumulation of water at low points (Pons et al., 2010; Dehotin et al., 2015; Zheng et al., 2018). 1D hydrological and hydraulic modelling approach, well established in the literature (Zhu et al., 2016; Rabori and Ghazavi, 2018; Sidek et al., 2021; Chahinian et al., 2023), are also applied to
40 simulate stormwater drainage network performance (Meng et al., 2019; Pla et al., 2019). Modelling platforms such as SWMM (Rossman, 2015; Rabori and Ghazavi, 2018) or InfoWorks ICM are 1D simulation tools applied in urban environments (Rubinato et al., 2013; Sidek et al., 2021). However, this type of modelling, which is essentially one-dimensional, does not provide spatial propagation of overflow water (Mark et al., 2004).. This aspect is taken into account by 2D models such as Mike Urban (DHI, 2021). The accuracy of the simulations they can provide on the spatial propagation of
45 surface flows is limited by both their numerical complexity, and the required data (fine topographic mesh, physical and urban characteristics) for their parameterization (Costabile et al., 2020; Zanchetta and Coulibaly, 2020). These 2D or coupled 1D-2D models (Martínez et al., 2018; Bulti and Abebe, 2020; Li et al., 2022) require substantial computing resources, long calculation times and are difficult to apply over large areas or for real-time flood forecasting studies (Rosenzweig et al., 2021). Today, the emergence of increasingly used AI (artificial intelligence) / ML (machine learning) techniques (Mosavi et al., 2018; Darabi et al., 2019), offers the possibility of providing flood mapping through model training (Mosavi et al., 2018; Darabi et al., 2019; Parvin et al., 2022; Taromideh et al., 2022). Their application can be challenging as they generally require a large amount of data (meteorological, hydrological, topographical) to be integrated for training, to improve accuracy and achieve good model performance (Bentivoglio et al., 2022).
50

In urban environments, one of the main factors influencing the choice of an appropriate modelling approach is data
55 availability (Henonin et al., 2013). In the African context, where the availability of detailed data is scarce, the challenge is to implement alternative solutions by finding a compromise between the availability of basic data, the reduction of calculation times, and the accuracy of flood simulations (Chahinian et al., 2023). This study aims to propose fine-resolution (25m²) modelling of flows and overflows from drainage and storage network over a large area (~400 km²) in Dakar urban periphery, with short calculation times (5mn) compatible with real-time applications. The proposed methodological approach follows
60 three main stages: (i) reconstruction of urban drainage directions, taking into account the modifications caused by the various urban developments (buildings, artificial channels, and retention basins), using algorithms developed for this purpose, (ii)

65 calculation of flows from small elementary catchments, using a parsimonious hydrological model (SCS-LR) adapted to the local context, which in particular integrates the density of urbanization, combined with (iii) a 1D hydraulic model for propagating these flows through the drainage network and a storage model for retention basins. The overflow points are identified by the difference between the maximum flows produced and the network capacity to evacuate them. This work is structured in four parts. First, the study area and the used datasets are described, then the detailed structure of the method is presented, followed by the model parameterization strategy and finally, two examples of simulation using a 10 and 100-year design storm are given and discussed highlighting possible improvements, before concluding.

2 Study area and datasets

70 2.1 Study area

The study area is located in the peri-urban of Dakar (Fig. 1a), capital of Senegal. This part of the city is characterized by a relatively flat relief (Fig. 1b), consisting of a series of small coastal dunes interspersed with wet depressions - called *Niayes* - that have dried up during the drought of the 1970s in the Sahelian zone (Nicholson et al., 2000). In the study area, the natural drainage network is temporary and has largely fossilized (Bassel, 1996). A major part of the soils is sandy in the dunes. 75 Hydromorphic soils dominate the area around the depressions (Fig. 1c) given the proximity of the water table in some places (Cissé Faye et al., 2004).

Dakar experiences extreme variations in monthly rainfall throughout the year. The rainy season last for 4 months, from June to September. August and September receive the highest amount of rain. Over the period 1988 to 2018, annual rainfall varies between 161 mm and 660 mm, with an average of 402 mm which is a characteristic of a tropical semi-arid zone. The 80 urbanization of this peri-urban area took place rapidly since, a few decades. It was largely fuelled by the rural exodus (Lericollais and Roquet, 1999) following the drought of the 1970s (Nicholson et al., 2000). This resulted in rapid population growth and a dense occupation of space helped by the establishment of the network of roads to facilitate urban mobility (Ndiaye, 2015). Moreover, settlement is sometimes achieved through (i) the infilling of former drained wetland depressions (Sène et al., 2018), (ii) self-occupation practices, without considering the topography of the land, the hydrology or the 85 installation of rainwater drainage structures (Ndiaye, 2015).

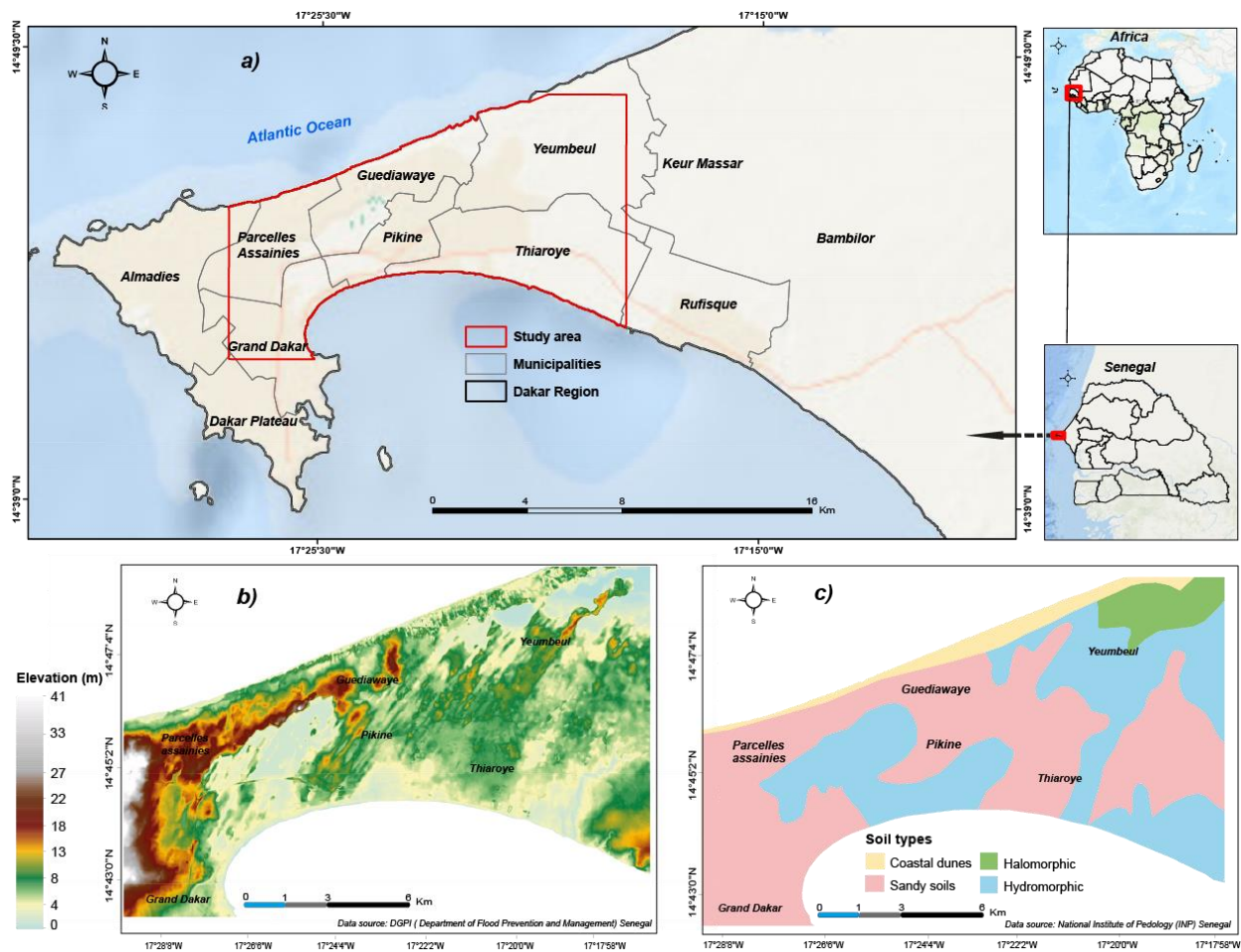


Figure 1: a) Location of the study area; b) Digital Terrain Model (DTM); c) soil type distribution

From the 2000s onwards, there was a return of rainfall (Sene and Ozer, 2002; Bodian, 2014; Nouaceur, 2020) after a period of drought, causing a series of floods in Dakar (Bottazzi et al., 2018; Hungerford et al., 2019). The most significant episodes are generally noted during the critical rainy periods in August and September: august 2005, September 2009, August 2012; August 2015, September 2020, August 2021, and recently August 2022. On 26 August 2012, for example, 161 mm of rain fell in less than 2 hours, including 144 mm in 51 minutes (Descroix et al., 2013) which had serious impact on the population, resulting in 26 deaths (Sané et al., 2016) and causing pandemics such as cholera and malaria (Sambe-Ba et al., 2013). One of the government's responses was to set up a vast program, including the Stormwater Management and Climate Change Adaptation project (PROGEP), which since 2012 has aimed to build drainage networks linked to storage basins to minimize the risks (Diop, 2019).

One of the current challenges for urban management, in the context of increasing intense rainfall, dense urbanization and infrastructure development, is to develop effective and robust tools to support flood assessment and decision-making.

100 2.2 Datasets

2.2.1 Geographic datasets

The geographical datasets required to reconstruct the modified urban drainage directions (Diémé et al., 2022) are compiled in an urban database for Dakar by the Senegal Flood Prevention and Management Department (DPGI) and the Geography and Cartography Department (DTGC). These include the DTM, the location of buildings, rainwater channels, and retention
 105 basins. The 10m resolution DTM, that we resampled to 5m, is specifically produced for the city of Dakar by the National Institute for Geographic and Forestry Information (IGN) of France, using the photogrammetric restitution technique. The buildings layer was created by manually digitizing high-resolution (50 cm) satellite images. The location and characteristics of the channels (width, depth) and retention basins (storage volume, leakage rate) are provided in the various technical reports supplied by the PROGEP project. The majority of channels are surface drains and are rectangular. All the known
 110 characteristics of the channels and the dimensions of the retention basins have been referenced for use in calibrating the hydraulic models.

2.2.2 IDF curves

The available IDF curves used in this study were derived from the GEV law parameters calculated by Sane et al. (2018), for each region of Senegal using long-term historical rainfall data from 23 tipping bucket rain gauges (Bodian et al., 2016).
 115 These historical data range from 1955 to 2005. To obtain a reliable estimate of the GEV distribution parameters μ , σ and ε for each rainfall station, all the rainfall of different durations d were merged, considering that the rainfalls of any duration d are identically distributed with a scaling factor η . This approach made it possible to estimate the GEV parameters (Eq. 1, 2, and 3) of the distribution of the rainfalls of any duration d as:

$$\mu(d) = \mu \cdot d^\eta \quad (1)$$

$$120 \quad \sigma(d) = \sigma \cdot d^\eta \quad (2)$$

$$\varepsilon(d) = \varepsilon \quad (3)$$

with $\mu = 28.9$ mm, $\sigma = 12.5$ mm, $\varepsilon = 0.08$, with η set to $\eta = -0.86$.

Application of Eq. 4 allow to determine a value x knowing his return period T .

$$x = \mu + \frac{\sigma}{\varepsilon} \left(-1 + \left(-\text{Ln} \left(1 - \frac{1}{T} \right) \right)^{-\varepsilon} \right) \quad (4)$$

125 For different return period (years), the rainfalls of duration d between 1 and 24 hours were then given by Table 1

Table: Summary of Dakar IDF curves calculated from GEV parameters defined by Sane et al. (2018).

Duration (hrs)	Return period (yrs)					
	2yr i_T mm/hr	5yr i_T mm/hr	10yr i_T mm/hr	20yr i_T mm/hr	50yr i_T mm/hr	100yr i_T mm/hr
1	34.4	49.7	60.6	71.7	87	99.3
2	18.9	27.2	33.1	39.1	47.5	54.2
4	10.3	14.8	18.1	21.4	25.9	29.5
6	7.2	10.4	12.7	15	18.2	20.7
9	5.1	7.3	8.9	10.5	12.7	14.5
12	4	5.7	6.9	8.1	9.9	11.2
24	2.1	3.1	3.8	4.5	5.5	6.3

3 Method presentation

The detailed methodological approach is structured in seven successive steps (Fig. 2). The first step is (i) the construction of the natural drainage topology modified by urban objects, (ii) on which is based the division of the urban area into small elementary catchment areas and the extraction of the associated hydrographic network. Then (iii) a rainfall-runoff model is applied to calculate the hydrographs at the outlets of the elementary catchment. These hydrographs are (iv) propagated in the stormwater drainage network by a 1D hydraulic model and (v) their storage in the retention basins is managed by a linear reservoir model. Finally, (vi) design storms are derived from local Intensity-Duration-Frequency (IDF) curves and used as input data to the model, which is then (vii) implemented to detect, over the entire study area, the overflow points of the drainage and storage network according to different levels of severity and urban density.

The modelling chain was built in the ATHYS platform, developed by Hydrosiences Montpellier. ATHYS enables a range of hydrological and hydraulic GIS-based models (MERCEDES unit), as well as geographical (VICAIR unit) and hydrometeorological (VISHYR unit) data processors. ATHYS is a free software, available from www.athys-soft.org. The entire processing chain and the associated data are presented in detail in the following sections.

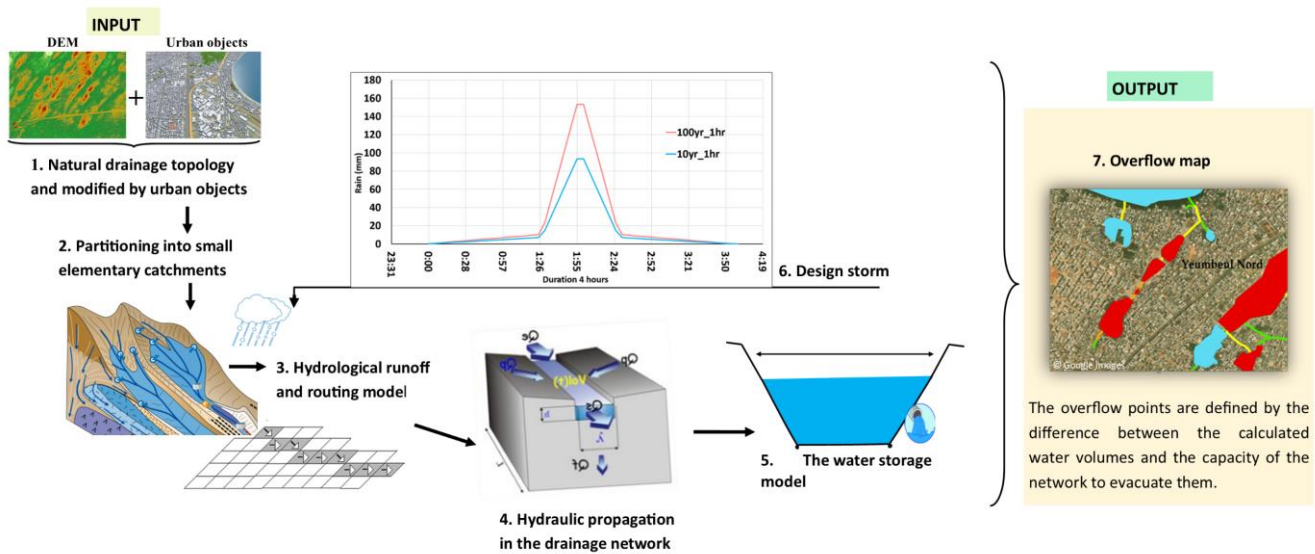


Figure 2: Flow chart of the methodology

3.1 Construction of the drainage topology

The construction of the drainage topology, which aims at reconstructing the modified drainage directions of runoff water, is a prerequisite to the implementation of the overflow point detection model. The natural path flows can be easily derived from the 5m-DTM, but in urban areas, the natural flows must be modified by artificial objects such as buildings, channels, and retention basins. This topology construction methodology was previously applied to the study area (Diémé et al., 2022), and can be summarized in 3 steps :

- a) modification of the elevation of the urban blocks (e.g. 25m) and extraction of the flow paths from the modified 5m-DTM (Jenson and Domingue, 1988),
- b) modification of flow paths according to the artificial channel network: The VICAIR algorithm uses a raster map of the channels, detects all the nodes of the channel network, and modifies the flow paths of each channel from the upstream node to the downstream node. The upstream and downstream nodes are recognized by their elevation in the DTM
- c) modification of the flow paths in the retention basins: The VICAIR algorithm uses a raster map of the basins, detects the outlet of the basin as being the channel that drains out the basin, and modifies all the flow paths of the basin towards the outlet.

3.2 Partitioning the study area into elementary catchments and networks

The modified drainage model was first used to reconstitute elementary catchments and channel networks. Building elementary catchments and channel networks is necessary to save time on computation as well as connect both hydrological

and hydraulic models. The elementary catchments were defined as catchments with the same urbanized area. A threshold of 10 hectares (ha) was adopted for this urbanized area. Thus catchments can be small (10 ha if totally urbanized) or larger (if the catchment is mostly natural). This allows to reduce the number of elementary catchments in the natural areas, without loss of accuracy regarding the channel network behaviour in the urban areas.

165 The criteria for delineating these catchments are taken from Jenson and Domingue (1988). They consist of marking the mesh as the outlet of a basin if:

- its urbanized drained area is greater than N (here 10ha)
- the difference in urbanized drained area between this mesh and the downstream mesh is greater than N.

Thus, 890 small urban catchments were delineated (Fig. 3a). The hydrographic network linking these small catchments was defined as all the meshes draining at least an area equal to 1 ha (Fig. 3b). For this network, we differentiated between meshes with known geometric characteristics (widths and depths of the main channels, i.e. 297 sections) and those with unknown characteristics (either natural sections or sections with unknown dimensions). The retention basins can be inserted in the channels network. Each retention basin is reduced to a single mesh, representing its outlet. To this mesh is assigned a height-volume-drainage law to describe the operation of the reservoir (see section 4.3).

175

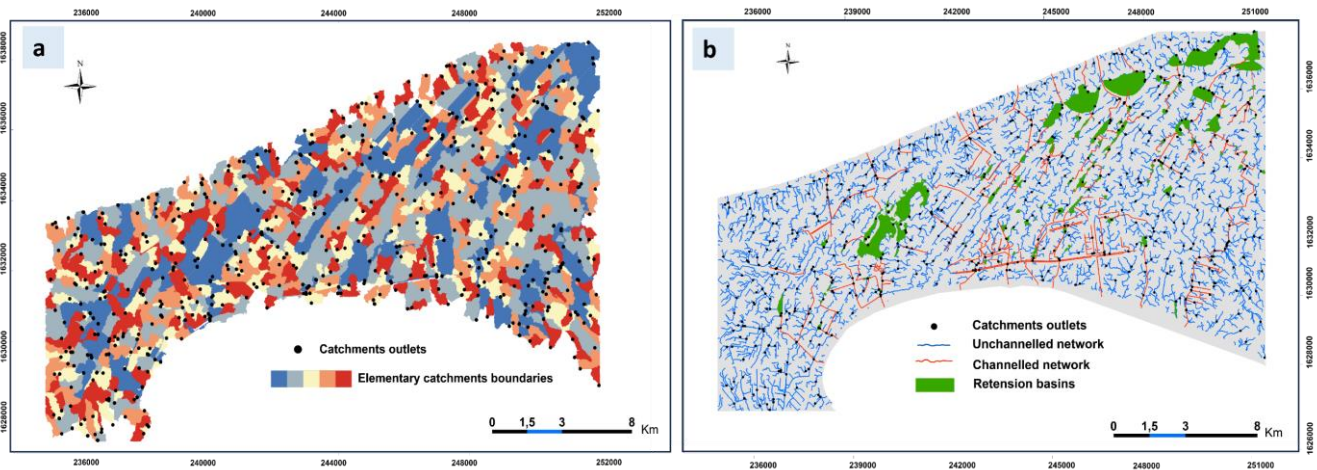


Figure 3: a) Partitioning of the area into small urban catchment; b) Definition of runoff transfer and storage classes

3.3 Application of hydrological runoff and routing model

3.3.1 The SCS (Soil Conservation Service) runoff model

The SCS hydrological model (Ponce and Hawkins, 1996), which is often applied in small urban catchments (Bouvier et al., 2018; Meng et al., 2019), was used to estimate the runoff on each mesh (Maref and Seddini, 2018; Bouadila et al., 2023). This model enables an increase of the runoff coefficient as a function of the cumulated rainfall with the main parameter to be determined as a function of soil type and land use, land use density, initial moisture conditions (Steenhuis et al., 1995; Huang et al., 2007).

The model parameters are I_a and S (or its CN equivalent). The parameter I_a represents the initial losses before the onset of runoff (mm), and S is the maximum water retention capacity of the soil at the start of the event (mm). The model is generally applied assuming that $I_a = 0,2.S$, and is expressed by Eq. (5):

$$Q = \frac{(P-0,2.S)^2}{P+0,8.S} \quad P > 0,2.S ; \text{ if not } Q = 0 \quad (5)$$

where P is the total rainfall during the event (mm), Q is the runoff during the event (mm).

The dynamic formulation of this model (i.e. the temporal evolution of the flow during the event) is given by Eq. 6, derivating Eq.5 in respect with time:

$$Pe(t) = Pb(t) \cdot \left(2 - \frac{(P(t)-0,2.S)}{P(t)+0,8.S} \right) \left(\frac{P(t)-0,2.S}{P(t)+0,8.S} \right) \quad (6)$$

Where $Pe(t)$ represents the runoff produced at time t (mm/h), $Pb(t)$ is the intensity of the rain at time t (mm/h), and $P(t)$ the cumulative rainfall at time t , since the start of the storm (mm). S is the only model adjustment parameter. The model is applied to each grid cell in the area with a time step of 5 minutes, S is likely to vary spatially depending on urban conditions.

3.3.2 The routing model

From each grid cell, the runoff provided by the SCS model is transferred to the outlet of an elementary catchment by the Lag and Route (LR) model (Fig. 4). Each cell provides an hydrograph at the outlet of the elementary catchment, and the complete hydrograph at the outlet of the elementary catchment is obtained by summing the cell hydrographs (Tramblay et al., 2011).

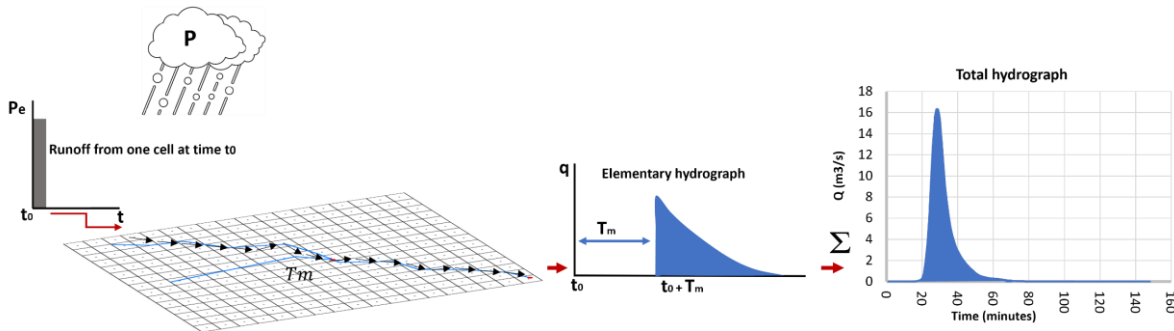


Figure 4: Conceptual diagram of the Lag and route model.

The cell hydrograph depends on 2 variables:

- the transfer time T_m (Eq. 7) from the mesh to the basin outlet, equal to:

$$T_m = L_m/V_o \quad (7)$$

205 where L_m is the distance from the mesh to the outlet, V_o is the average velocity of the flow between the mesh and the outlet traveled (possibly varying for each mesh)

- the time K_m (Eq. 8) associated with the diffusion of the flood wave during the transfer time T_m , equal to:

$$K_m = K_o \cdot T_m \quad (8)$$

where K_o is the proportionality coefficient between diffusion (lag) and translation (route).

V_o and K_o are the 2 parameters of the LR model.

210 The equation of the elementary hydrograph (Eq. 9) produced by the effective rainfall $Pe(t_o)$ obtained on each mesh at each time is given by:

$$Q(t) = \frac{Pe(t_o)}{K_m} \exp\left(\frac{t-(t_o+T_m)}{K_m}\right) A \quad \text{if } t > t_o + T_m \quad \text{and } Q(t) = 0 \text{ if not} \quad (9)$$

215 where A is the mesh size (here $25m^2$). The LR model has the advantage of being numerically stable in respect to both the cell size and the computation time step, allowing fast calculation times, as used here, with cell size $25 m^2$ and time step $5mn$.

3.4 The propagation model in the drainage network

The hydraulic propagation of flow in the unchanneled network and the channeled network (297 collectors) is computed by the 1D Kinematic Wave (KW) model (Constantindes, 1981). The KW model combines a conservation equation (Eq. 10):

$$\frac{\partial A}{\partial t} + \frac{\partial Q}{\partial x} = 0 \quad (10)$$

220 where Q is the flow rate (m^3/s), A is the area of the wetted cross-section (in m^2), x is the horizontal distance (m) and t is the time (s) ;

with a dynamic equation, used as the Manning-Strickler formula (Eq. 11) :

$$V(t) = K_r \cdot \sqrt{S_f} \cdot R_h^{2/3} \quad (11)$$

225 where $V(t)$ represents the flow velocity ($m \cdot s^{-1}$), K_r the Manning Strickler roughness coefficient ($m^{1/3} \cdot s^{-1}$), R_h (m) the hydraulic radius calculated from the channel's geometric characteristics (width λ and depth P_c), S_f . ($m \cdot m^{-1}$) the friction slope, using :

$$S_0 = S_f \quad (12)$$

where S_0 is the channel/ground slope ($m \cdot m^{-1}$).

230 To apply Eq. 11 to water flow in channels or surface runoff, it is assumed that the friction slope is equal to the bed slope (Eq. 12). The numerical stability of the KW model needs to respect the Courant's condition, which leads to computation with very short times (some seconds) when using elements of small size, typically 25 m^2 . It thus requires longer computation times to calculate the mesh-to-mesh flows in the channeled and unchanneled network. The time saving is obtained by limiting the calculations to the network meshes, which means a small number of meshes.

235 Considering that the channels have mostly rectangular shape, the parameters of the KW model for each channelled or unchanneled cell of the drainage network are K_r the Manning-Strickler coefficient, λ the width of the rectangular cross-section, P_c the depth of the rectangular cross-section. The slopes of the cells can be derived from the DTM, see 4.2.

3.5 The water storage model in retention basins

240 Modelling the water storage in the retention basins is based on the principle that the retention basin is reduced to only one cell, which figures the basin outlet. This cell must have specific characteristics which must emulate the behaviour of the basin (Table 2). These characteristics are the storage (in millions of cubic meters) in the basin and the outflow rate (in cubic meters per second) at different tabulated water levels (in m) :

Table 2: Example of a reservoir operation

Water level (m)	Volume ($10^6 \cdot \text{m}^3$)	Outflow (m^3/s)
0	0	0
H_1	V_1	Q_1
....
H_{\max}	V_{\max}	Q_{\max}

245 where the first line is associated to the minimal storage in the basin, and the last line is associated to the maximal storage in the basin. When the maximal storage is reached, the inflow rate is added to the outflow rate. It is supposed that volumes and outflows vary linearly between 2 lines.

A specific case, with only 2 lines (1 for the minimal storage, 1 for the maximal storage), emulates a linear reservoir model for all the water levels in the basin, see 4.3.

250 4 Model calibration

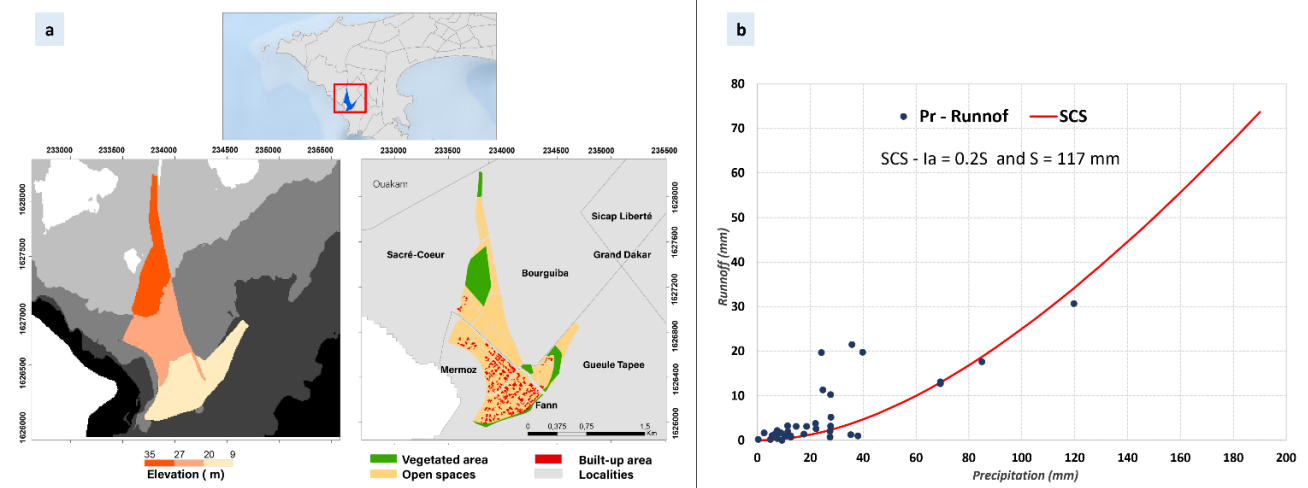
Implementing the model on the whole study area requires calibration of the parameters: (i) S for the SCS model, (ii) the V_0 and K_0 for the LR model, (iii) K_r , λ and P_c for the 1D Kinematic Wave model, (iv) the storage capacity and discharge rate at the outlet of each reservoir for the storage model.

4.1 Calibration of the rainfall-runoff model

255 4.1.1 Calibration of the SCS runoff model

To calibrate the hydrological model, we first estimated the infiltration rates on the very sandy soils often found in Dakar using inverse modelling of soil moisture measurements in relation to rainfall (Le Bourgeois et al., 2016). Tests carried out using Hydrus 1D software (Šimůnek et al., 2016) showed that these soils were highly permeable and capable of infiltrating rainfall in full (Diémé, 2023).

260 We then used hydrological data available for the city of Dakar (Fig. 5b) and measured in the Fann Mermoz experimental catchment by Bassel et al. (1994) and Bassel and Pépin (1995). Both observed rainfall and runoff data make it possible to evaluate the runoff coefficients for different rainfall events (Fig. 5b) in this experimental catchment, where the built-up coefficient was approximately 20% (Fig. 5a).



265 **Figure 5: a) Characteristics of the Fann Mermoz experimental basin; b) Relationship between rainfall and runoff (data taken from Bassel, 1996).**

The estimated runoff coefficients are of the order of 10% for a rainfall of 40 mm, 20% for a rainfall of 78 mm, and 30% for a rainfall of 150 mm. In other words, the built-up coefficient of the catchment is close to the runoff coefficient associated with a rainfall of 78 mm, i.e. a rainfall with a ten-year return period in Dakar (Sane et al., 2018). This is consistent with the filtering nature of the soil, as we have characterized, which indicates that unpaved soils produce negligible runoff for most rainfall events. To obtain a runoff coefficient of 20% with a rainfall of 78mm, the value of the S parameter of the SCS model must be set to 117mm.

270 Finally, we generalized the assumption that the building coefficient is equal to the runoff coefficient associated with a ten-year rainfall for the entire Dakar site. The build-up coefficients were calculated for each urban block, as the ratio of the surface area of the buildings to the surface area of the block (Fig. 6). All the meshes within the same urban block were then assigned the value calculated for the block.

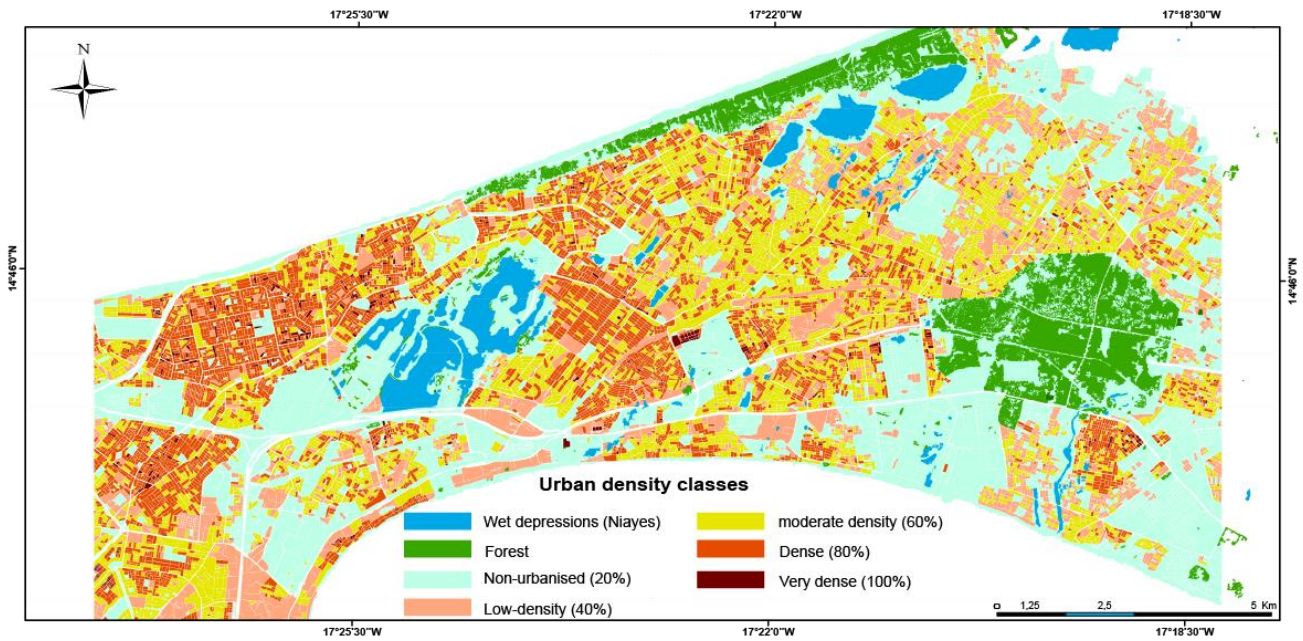


Figure 6: Determination of urban density classes by urban block

Finally, we calculated the values of S for different classes of building coefficient, following Eq. (13):

$$280 \quad CR = \frac{Q}{P} = \frac{(P-0.2S)^2}{P \cdot (P+0.8S)} \quad (13)$$

Where P is the height of the 10-year rainfall in 4 hours, i.e. 78 mm. The values obtained after adjusting the S parameter are shown in Table 2.

Table 2: Summary of values obtained for the S parameter of the SCS model

Urban density classes %	Runoff coefficient (ten-yearly)	S values
20	20	117
40	40	67
60	60	35
80	80	15
100	100	0

4.1.2 Calibration of the routing model

285 The Ko parameter was set at 0.7, the empirical value usually used (Bouvier et al., 2017). The Vo parameter was determined by using historical data from the Fann Mermoz experimental catchment (Bassel, 1996).

Based on the observed data of this study, the lag-time T_r (between the center of gravity of the runoff and the center of gravity of the rainfall) could be estimated to be 30 mn. We considered that this lag-time should be the same as the one provided by the LR model, applied to the mesh occupying the center of gravity of the catchment active zone (urbanized area). This mesh is located approximately 1.2 km from the basin outlet. The theoretical response time provided by the model is given by Eq. (14):

$$T_r = T_m + K_m \quad (14)$$

With m the mesh of the center of gravity of the catchment, this leads to Eq. (15):

$$T_r = 1.7 T_m = 1.7 L_m/V_o \quad (15)$$

And therefore V_o is obtained using Eq. (16):

$$V_o = 1.7 L_m/T_r \quad (16)$$

Applying Eq. 16 with $T_r = 30$ mn and $L_m = 1.2$ km leads to $V_o = 1.1$ m/s.

This estimation based on data from the experimental catchment was then extrapolated to the whole study area, considering the velocity V_o to be uniform and equal to that obtained for the Fann-Mermoz catchment for all rainfall events. This approximation is justified by the fact that slopes vary little in Dakar, and are on average fairly close to those of the Fann-Mermoz catchment.

4.2 1D hydraulic model calibration

4.2.1 Propagation in the unchanneled network

The unchanneled network meshes here have been linked to both (i) the right-of-way of streets and roads which, in urbanized areas, become the transfer pathways for surface runoff (Zhang et al., 2018; Skrede et al., 2020) due to the presence of buildings, walls and other urban objects (Fig. 7) that divert flows (Diémé et al., 2022) and (ii) the shallow natural reaches arising from non-urbanized surfaces. unchanneled



Figure 7: Surface water drainage paths at urban street level.

The network meshes derived from streets and roads were classified into types (residential streets, primary-secondary roads, national roads, and freeways), and assigned a specific width according to their spatial footprint. This was done interactively, on-screen, by superimposing the city's roads and streets layer onto a satellite imagery background (Google Earth). The widths (λ) corresponding to each category of the road were estimated on a case-by-case basis, taking considering the alignment of the carriageway and its verges. Figure 8 shows the values found (in meters) and defined using Google Earth's distance measurement tools. As there are no constraints (walls, partitions, etc.) in the propagation of natural reaches, they have been considered in the model as having infinite width.



320 **Figure 8: Determining the widths of unchanneled transfer classes**

About the depth of the minor bed (P_c) associated with street and road meshes, an infinite depth has been set, so that the flow remains channeled by the width of the road or street (in this case by the walls bordering the street) and considered to be null for the meshes of the natural reaches, which are very little marked in Dakar. Manning Strickler roughness coefficients were estimated at $50 \text{ m}^{1/3} \cdot \text{s}^{-1}$ for all street and road meshes with more or less smooth surfaces, and at $20 \text{ m}^{1/3} \cdot \text{s}^{-1}$ for natural meshes with rough surfaces.

Slope values were calculated from the DTM, using the differences in elevation at the nodes of each mesh, in the mesh's drainage direction, then smoothed, to limit the sensitivity of the 1D Kinematic Wave model to slope variability (sometimes linked to DTM accuracy shortcomings). Smoothing was based on the difference between the altitudes of the mesh and the N^{th} mesh downstream, divided by the length of the trajectory between the mesh and the N^{th} mesh downstream. The number N of meshes used for smoothing has been set at 50 meshes. If the calculated slope is equal to 0 (or even <0) or there is no N^{th} mesh (on the edges of the image), this slope is assigned the value 0.001 m/m. Slopes smoothed in this way range from 0.001 to 0.4 m/m, with an average of 0.007 m/m.

4.2.2 Calibration of the propagation model in the channeled network

The parameters λ and P_c , used to calculate the hydraulic radius, were set based on the dimensions of the collectors for which information on their characteristics (width and depth) is available in the preliminary and detailed technical reports produced as part of PROGEP. The roughness coefficient has been uniformly set at $50 \text{ m}^{1/3}\text{s}$, and flows are calculated over all channel sections, taking into account the overall rectangular cross-section. The slopes applied are obtained by smoothing the DTM altitudes as indicated above.

4.3 Calibration of the water storage model

All the retention basins were considered having regular shapes where the volume and the water level were proportional. They also were considered as having a linear reservoir behaviour, so that the outflow and the storage volume (or the water level) are also proportional. Thus, the volume-water level-outflow can be reduced to only 2 lines, where the upper line denotes the lowest volume, water level, and outflow in the basin, and the lower line the highest volume, water level, and outflow in the basin. For example, a basin that has $15\,000 \text{ m}^3$ maximal volume, 1.2 m maximal water level, and $3.90 \text{ m}^3/\text{s}$ maximal outflow will be associated with table 2.

Table 2: Example of a reservoir operation

Water level (m)	Volume (10^6 m^3)	Outflow (m^3/s)
0	0	0
1,2	15 000	3,90

From this table, each value of water level or outflow corresponding to a given volume is linearly interpolated between the minimal and the maximal storage volumes. When maximum reservoir storage value is reached, the inflow entering the reservoir is fully transferred downstream as outflow.

In the list of retention basins (106), only the retention basins built as part of the PROGEP project (84 basins) have detailed information (storage capacity, maximum water level and discharge rate), which we have extracted from the various reports produced by this project. As for the other basins whose dimensions are not known, we have assigned them, by default, characteristics based on a criterion of similarity of the shapes of their contours with those of basins whose dimensions are known, and by visually comparing them using satellite imagery from Google Earth.

5 Modelling of the drainage overflow

5.1 Design storms construction

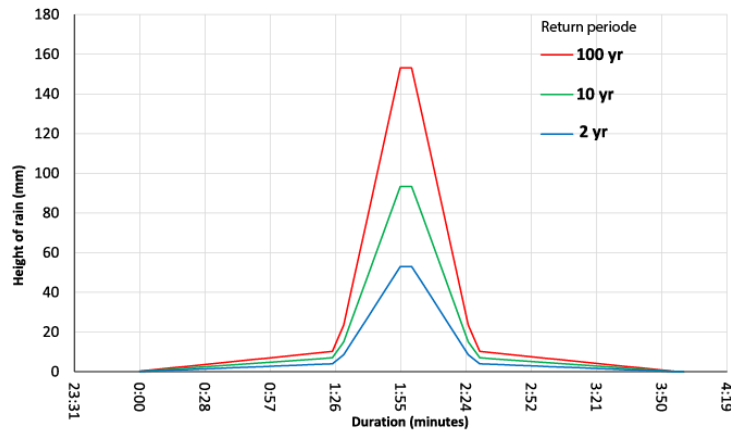
Design storms (Fig. 9) were constructed to be used as input data for the model to simulate runoff discharges (Zhenyu and Olivier, 2005; Balbastre-Soldevila et al., 2019).

360 The maximum rainfall provided by the IDF curves (table 1), was used to construct the design storms. The design storm model used is the double triangular rainfall model proposed in France by Desbordes and Raous (1976). It takes into account: (i) the total duration of the rain, t_3 , whose height taken from the IDF is equal to $P(t_3, T)$, (ii) the period of intense rain of duration t_1 , whose height $P(t_1, T)$, is also taken from the IDF and (iii) a period t_2 (here $\frac{t_3 - t_1}{2}$ in case of a symmetric design rainfall) which constitutes a period of rain before and after the intense period. For its construction, the basic parameters to be
 365 determined are i_m (the maximum intensity before the intense period) and i_M (the maximum intensity of the peak of the intense rainfall). They are calculated following Eq. (17 and 18):

$$i_m = \frac{P(t_3, T) - P(t_1, T)}{t_2} \quad (17)$$

$$i_M = \frac{2P(t_1, T)}{t_1} - i_m \quad (18)$$

To build the design storm for different return periods, we selected a total duration $t_3 = 4\text{h}$ generally observed in African
 370 convective systems (Tadesse and Anagnostou, 2010). The, duration of the intense rainfall t_1 must be related to the time of concentration of the catchments; we chose $t_1 = 1\text{h}$ according to the transfer time over the largest catchments. Other attempts using 30 mn and 10 mn do not show significant differences in the flow discharges at the outlet of the catchments, whatever size they have.

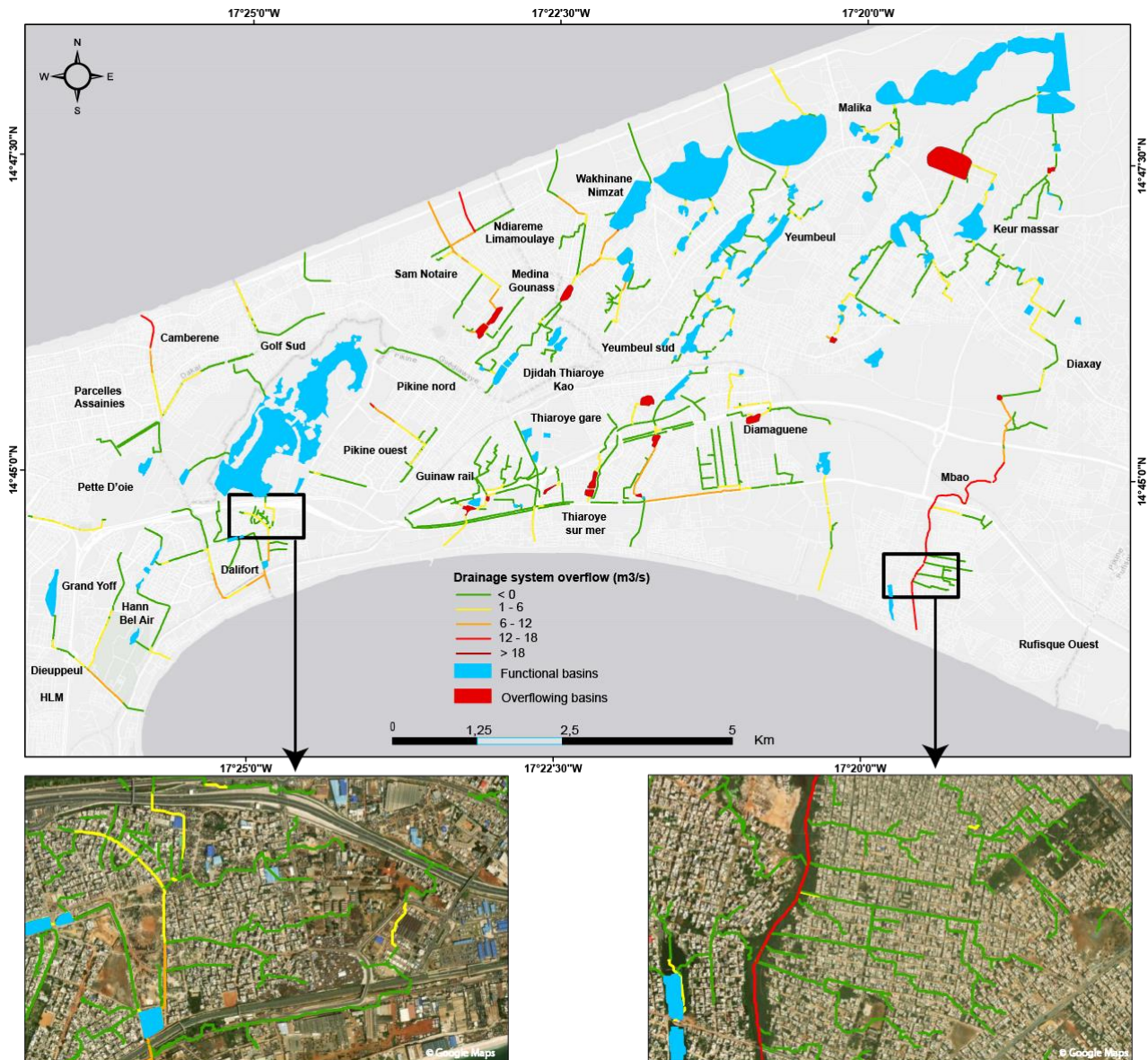


375 **Figure 9: Construction of the design storms for return periods of 2, 10 and 100 years with an intense period of 1 hour and 4 hours total duration.**

5.2 Implementation to detect network overflows

Running the simulation model provides the flows, heights and velocities in the drainage and storage networks throughout the event. The overflows from the network correspond to a positive difference between the simulated flows and the full-load
 380 capacities for the drainage network, and to a positive difference between the simulated volume and the maximum volume for the storage basins. The capacities of the drainage network were calculated by applying the Manning-Strickler formula at full load, i.e. with a head of water corresponding to the depth of the structure. The results are maps of overflows from the

stormwater drainage network and retention basins at the scale of the study area. The results presented here are based on running the model with 10-year (78 mm; Fig. 10) and 100-year (128 mm; Fig. 11) design storm over 4 hours. The simulations were carried out on the assumption that the rainfall was uniform over all the defined catchment areas. The simulations carried out show that the network records significant overflows for rainfall with a 10-year return period, with overflow levels ranging from 1-12 m³/s for some sections and until 18 m³/s for three sections. For most of the collectors that overflowed, the overflow rate varied between 1 and 6 m³/s.



390 **Figure 10: Identification of network overflow points for a 10-year return period rainfall.**

Beyond the ten-year rainfall frequency, the network shows widespread overflow levels. This applies to both collectors and storage basins. However, some reservoirs are still operational. The large natural depressions (the Niayes) do not overflow. Overflows are noted on a large proportion of the collectors, with thresholds sometimes exceeding $18 \text{ m}^3/\text{s}$ in some cases. The simulations also show that the flow load has caused a large number of retention basins to overflow.

395



Figure 11: Identification of network overflow points for a 100-year return period rainfall.

5.3 Discussion

The model used in this study has the advantage of being relatively simple and is capable of covering an entire city with a fine resolution (5m^2) and short calculation times (typically 5 minutes). This makes it a useful tool for assessing flood risk. The model is also compatible with real-time flood forecasting applications if remote rainfall data is available. However, this study has a number of limitations. An important factor is the construction of the drainage topology based on the DTM, which has focused solely on the effects of the location of buildings, canals, and storage basins in modifying drainage directions. To obtain a more detailed view, the analysis should be extended to include other urban objects that influence the trajectories of surface runoff flows. Future work will focus on lidar data (currently being compiled for the Dakar region), which provides more detail than DTM on urban micro-objects and could thus be used to refine the reconstruction of induced drainage directions.

The other limitation of this work relates to the availability of the data (hydrological, hydrometric, or piezometric) required to calibrate the hydrological runoff-routing models (SCS-LR) applied to this drainage topology to calculate flows. In this study, the calibration of the SCS runoff model was based on the hypothesis established from short series of data from the Fann Mermoz experimental basin, by considering that the ten-year runoff coefficient is equal to the building coefficient. Although this simplification may be acceptable for the case of Dakar, where soils are generally sandy and very permeable (Diémé, 2023), new data must be produced to verify the hypothesis. In other cities where the soils are less permeable, direct (Kelleners et al., 2005) or indirect (Galagedara et al., 2003) infiltration measurements on several representative sites should be used as a basis for determining the contribution of these soils to surface runoff. A particular constraint is the influence of the rising water table in Dakar (Faye et al., 2019), which must be taken into account in the flow generation model. One possible solution is to obtain piezometric data giving the water table level and reduce the S parameter of the SCS model on the meshes corresponding to outcrops of the water table. The rainfall data used as input to the model was applied on the assumption that the rainfall was uniform over all the defined catchment areas. Such a hypothesis does not account for the areal reduction factor, but can be adopted because most of the catchments (i.e. 94%) have small areas, less than 2 km^2 . The largest catchment areas account for 4% (2 to 6 km^2) and 2% (6 to 12 km^2) out of the 890 catchment outlets which have been considered. Also, to take better account of the extreme precipitation regime, it would be interesting, instead of stationary IDF curves (used in this study), to explore non-stationary statistical methods for determining IDF curves (Chagnaud et al., 2021) that incorporate the uncertainties associated with climate change. Likewise, a good integration of the spatial variability of precipitation is necessary for more accurate surface water runoff simulation. Alternative and innovative methods based on rainfall estimation using microwave links from cellular communication networks (Turko et al., 2021; Djibo et al., 2023) are currently being tested in African cities where the coverage of rainfall measurement stations is poor.

About the LR routing model, it was calibrated by considering the transfer velocity (V_0), calculated on the Fann Mermoz experimental basin, as uniform over the entire study area. The slope conditions, which vary little in the study area, allow us to retain this approximation. It is clear that the calibration of both the SCS-LR runoff-routing models needs to be improved

using new experimental data, which is relatively rare in African cities. This should motivate the setting up of new experimental sites, in order to better estimate the parameters of the flow calculation models. Additionally, one of the improvements to be made to the model concerns the calculation of the slopes used by the KW hydraulic model to ensure the propagation of flows in the channeled and unchanneled network. A simplification has been applied, involving smoothing to
435 reduce the sensitivity of the KW model to irregular variations in the slope of the terrain, sometimes linked to a mistake in the DTM. The availability of lidar data in the study area will enable us to compare the model's performance using more accurate slopes. Similarly, the congestion of collectors (household waste, silting, etc.) can be incorporated into the hydraulic model. This could be taken into account by reducing the cross-section of the collector, even if information on this congestion is difficult to obtain.

440 Finally, validating the results of the model simulations is one of the major perspectives of this study. As things stand at present, it was not possible to get the necessary data for the validation of the method, which means on the one hand sub-daily rainfall data, and on the other hand flood maps for the recent events that occurred in Dakar. The imminent installation of a rain gauge radar in Dakar could help to facilitate this. Flood maps could be obtained by exploring citizen science tools(Sy et al., 2020), using information on feedback, recent flooding situations, and data on the intensity of rainfall events that cause
445 flooding as applied to Bamako (Mali)by Chahinian et al. (2023), or order a high-precision satellite image to map out flooded areas. Validation of the method would enable it to be extended to other towns and cities, thereby ensuring sound planning decisions.

6 Conclusions

A fine-scale simulation model of runoff over an entire urban area and an assessment of the response of the storm drainage
450 network (canals and retention basins) to different rainfall events has been developed. It is based on a preliminary reconstruction of the drainage directions modified by urbanization and the implementation of combined hydrological and 1D hydraulic models calibrated to the city's urban conditions.

The results obtained are overflow maps for the city's drainage network for rainfall intensities of different return periods. The representation of overflow points is associated here with one-dimensional modelling, but is still sufficiently informative to
455 guide the deployment of emergency services on the ground, or to initiate action at strategic locations: assessment of the effectiveness of planned developments, tests of different rainfall and urbanization scenarios, detection of overflows in near-real time with remote rainfall data. In addition, the model also provides boundary conditions for applying 2D hydraulic models to determine locally the propagation of overflows from stormwater drainage network over limited areas. Future work will focus on improving the availability of data to facilitate the assessment of simulation uncertainties and validate the
460 overflow results. Indeed, one of the challenges of urban hydrology in African cities is to set up urban databases that are essential for conducting relevant studies and for better characterizing and forecasting floods.

Data Availability

The data used in this article are available from the first author, LPM Diémé, upon reasonable request.

465 Author contribution

LPMD conceptualized and performed the draft preparation. CB implemented the codes on ATHYS software. AB contributed to data analysis. AS has provided Geographic datasets. LPMD, CB, and AB developed the methodology, provided the simulation and details about it. All authors were involved in reviewing and editing the paper.

Competing interests

470 The authors report no conflicts of interest.

Acknowledgements

This article was produced with the support of the Water Cycle and Climate Change (CECC) 2021-2025 project, co-funded by IRD and AFD. The authors would also like to thank the technical structures that agreed to make the data used in this article available.

475 References

- Agonafir, C., Lakhankar, T., Khanbilvardi, R., Krakauer, N., Radell, D., and Devineni, N.: A review of recent advances in urban flood research, *Water Secur.*, 19, 100141, <https://doi.org/10.1016/j.wasec.2023.100141>, 2023.
- Balbastre-Soldevila, García-Bartual, and Andrés-Doménech: A Comparison of Design Storms for Urban Drainage System Applications, *Water*, 11, 757, <https://doi.org/10.3390/w11040757>, 2019.
- 480 Barau, A. and Wada, A. S.: Do-It-Yourself Flood Risk Adaptation Strategies in the Neighborhoods of Kano City, Nigeria, in: *African Handbook of Climate Change Adaptation*, edited by: Oguge, N., Ayal, D., Adeleke, L., and da Silva, I., Springer International Publishing, Cham, 1353–1380, https://doi.org/10.1007/978-3-030-45106-6_190, 2021.
- Bassel, M.: *Eaux et environnement à Dakar-Pluies, ruissellement, pollution et évacuation des eaux. Contribution à l'étude des problèmes d'environnement liés aux eaux dans la région de Dakar*, PhD thesis, Université Cheikh Anta Diop de
485 Dakar, Département de Géographie, 244 pp., <https://www.documentation.ird.fr/hor/fdi:010012652> (last access: 20 October 2023), 1996.

- Bassel, M., and Pépin, Y.: Pluies, ruissellement, évacuation et qualité des eaux sur le bassin versant de Mermoz-Fann: Contribution à l'étude des problèmes d'environnement liés aux eaux dans la région de Dakar, rapport de campagne, ORSTOM, 59 pp., <https://www.documentation.ird.fr/hor/fdi:010010028> (last access: 20 October 2023), 1995.
- 490 Bassel, M., Pépin, Y., and Thiébaux, J. P.: Rapport de campagne: Bassin urbain de Dakar, ORSTOM, 55 pp., <https://www.documentation.ird.fr/hor/fdi:010020660> (last access: 27 October 2023), 1994.
- Bentivoglio, R., Isufi, E., Jonkman, S. N., and Taormina, R.: Deep learning methods for flood mapping: a review of existing applications and future research directions, *Hydrol. Earth Syst. Sci.*, 26, 4345–4378, <https://doi.org/10.5194/hess-26-4345-2022>, 2022.
- 495 Bichet, A. and Diedhiou, A.: West African Sahel has become wetter during the last 30 years, but dry spells are shorter and more frequent, *Clim. Res.*, 75, 155–162, <https://doi.org/10.3354/cr01515>, 2018.
- Bodian, A.: Caractérisation de la variabilité temporelle récente des précipitations annuelles au Sénégal (Afrique de l'Ouest), *Géographie Phys. Environ. Physio-Géo*, 8, <https://doi.org/10.4000/physio-geo.4243>, 2014.
- Bottazzi, P., Winkler, M. S., Boillat, S., Diagne, A., Maman Chabi Sika, M., Kpangon, A., Faye, S., and Speranza, C. I.:
500 Measuring Subjective Flood Resilience in Suburban Dakar: A Before–After Evaluation of the “Live with Water” Project, *Sustainability*, 10, 2135, <https://doi.org/10.3390/su10072135>, 2018.
- Bouadila, A., Bouizrou, I., Aqnouy, M., En-nagre, K., El Yousfi, Y., Khafouri, A., Hilal, I., Abdelrahman, K., Benaabidate, L., Abu-Alam, T., Stitou El Messari, J. E., and Abioui, M.: Streamflow Simulation in Semiarid Data-Scarce Regions: A Comparative Study of Distributed and Lumped Models at Aguenza Watershed (Morocco), *Water*, 15, 1602,
505 <https://doi.org/10.3390/w15081602>, 2023.
- Bouvier, C., Chahinian, N., Adamovic, M., Cassé, C., Crespy, A., Crès, A., and Alcoba, M.: Large-Scale GIS-Based Urban Flood Modelling: A Case Study on the City of Ouagadougou, in: *Advances in Hydroinformatics, SimHydro2017*, Sophia-Antipolis, France, 703–717, https://doi.org/10.1007/978-981-10-7218-5_50, 2017.
- Bouvier, C., Bouchenaki, L., and Tramblay, Y.: Comparison of SCS and Green-Ampt Distributed Models for Flood
510 Modelling in a Small Cultivated Catchment in Senegal, *Geosciences*, 8, 122, <https://doi.org/10.3390/geosciences8040122>, 2018.
- Bulti, D. T. and Abebe, B. G.: A review of flood modeling methods for urban pluvial flood application, *Model. Earth Syst. Environ.*, 6, 1293–1302, <https://doi.org/10.1007/s40808-020-00803-z>, 2020.
- Chagnaud, G., Panthou, G., Vischel, T., Blanchet, J., and Lebel, T.: A unified statistical framework for detecting trends in
515 multi-timescale precipitation extremes: application to non-stationary intensity-duration-frequency curves, *Theor. Appl. Climatol.*, 145, 839–860, <https://doi.org/10.1007/s00704-021-03650-9>, 2021.
- Chagnaud, G., Panthou, G., Vischel, T., and Lebel, T.: A synthetic view of rainfall intensification in the West African Sahel, *Environ. Res. Lett.*, 17, 044005, <https://doi.org/10.1088/1748-9326/ac4a9c>, 2022.

- Chahinian, N., Alcoba, M., Dembélé, N. D. J., Cazenave, F., and Bouvier, C.: Evaluation of an early flood warning system in Bamako (Mali): Lessons learned from the flood of May 2019, *J. Flood Risk Manag.*, <https://doi.org/10.1111/jfr3.12878>, 2023.
- Chen, Y., Zhou, H., Zhang, H., Du, G., and Zhou, J.: Urban flood risk warning under rapid urbanization, *Environ. Res.*, 139, 3–10, <https://doi.org/10.1016/j.envres.2015.02.028>, 2015.
- Constantindes, C. A.: Numerical techniques for a two-dimensional kinematic overland flow model., *Water SA*, 7, 234–248, 1981.
- Costabile, P., Costanzo, C., De Lorenzo, G., and Macchione, F.: Is local flood hazard assessment in urban areas significantly influenced by the physical complexity of the hydrodynamic inundation model?, *J. Hydrol.*, 580, 124231, <https://doi.org/10.1016/j.jhydrol.2019.124231>, 2020.
- Coulibaly, G., Leye, B., Tazen, F., Mounirou, L. A., and Karambiri, H.: Urban Flood Modeling Using 2D Shallow-Water Equations in Ouagadougou, Burkina Faso, *Water*, 12, 2120, <https://doi.org/10.3390/w12082120>, 2020.
- Darabi, H., Choubin, B., Rahmati, O., Torabi Haghighi, A., Pradhan, B., and Kløve, B.: Urban flood risk mapping using the GARP and QUEST models: A comparative study of machine learning techniques, *J. Hydrol.*, 569, 142–154, <https://doi.org/10.1016/j.jhydrol.2018.12.002>, 2019.
- Dehotin, J., Chazelle, B., Laverne, G., Hasnaoui, A., Lambert, L., Breil, P., and Braud, I.: Mise en œuvre de la méthode de cartographie du ruissellement IRIP pour l’analyse des risques liés aux écoulements sur l’infrastructure ferroviaire, *Houille Blanche*, 101, 56–64, <https://doi.org/10.1051/lhb/20150069>, 2015.
- Desbordes, M. and Raous, P.: Un exemple de l’intérêt des études de sensibilité des modèles hydrologiques, *Houille Blanche*, 62, 37–43, <https://doi.org/10.1051/lhb/1976004>, 1976.
- DHI (Danish Hydraulic Institute): Mike Flood 1D-2D and 1D-3D Modelling - user manual, 154 pp., https://manuals.mikepoweredbydhi.help/2021/Water_Resources/MIKE_FLOOD_UserManual.pdf (last access: 17 October 2023), 2021.
- Diémé, L. P.: Système de surveillance des inondations à l’échelle de l’agglomération de Dakar, PhD thesis, Université Gaston-Berger, Département de géographie, 177 pp., <https://doi.org/10.13140/RG.2.2.19319.09121> (last access: 29 October 2023), 2023.
- Diémé, L. P., Bouvier, C., Bodian, A., and Sidibé, A.: Construction de la topologie de drainage à fine résolution spatiale en milieu urbain: exemple de l’agglomération de Dakar (Sénégal), *LHB*, 108, 2061313, <https://doi.org/10.1080/27678490.2022.2061313>, 2022.
- Diop, L., Bodian, A., and Diallo, D.: Spatiotemporal Trend Analysis of the Mean Annual Rainfall in Senegal, *Eur. Sci. J. ESJ*, 12, 231–231, <https://doi.org/10.19044/esj.2016.v12n12p231>, 2016.
- Diop, M. S.: Les capacités adaptatives des communautés de la périphérie de Dakar face aux inondations, PhD thesis, Université Paris Saclay (COmUE), 354 pp., <https://tel.archives-ouvertes.fr/tel-02415826>, 2019.

- Faye, S. C., Diongue, M. L., Pouye, A., Gaye, C. B., Travi, Y., Wohnlich, S., Faye, S., and Taylor, R. G.: Tracing natural groundwater recharge to the Thiaroye aquifer of Dakar, Senegal, *Hydrogeol. J.*, 27, 1067–1080, <https://doi.org/10.1007/s10040-018-01923-8>, 2019.
- 555 Gaisie, E. and Cobbinah, P. B.: Planning for context-based climate adaptation: Flood management inquiry in Accra, *Environ. Sci. Policy*, 141, 97–108, <https://doi.org/10.1016/j.envsci.2023.01.002>, 2023.
- Galagedara, L. W., Parkin, G. W., and Redman, J. D.: An analysis of the ground-penetrating radar direct ground wave method for soil water content measurement, *Hydrol. Process.*, 17, 3615–3628, 2003.
- Goldsmith, P. D., Gunjal, K., and Ndarishikanye, B.: Rural–urban migration and agricultural productivity: the case of
560 Senegal, *Agric. Econ.*, 31, 33–45, <https://doi.org/10.1111/j.1574-0862.2004.tb00220.x>, 2004.
- Henonin, J., Russo, B., Mark, O., and Gourbesville, P.: Real-time urban flood forecasting and modelling – a state of the art, *J. Hydroinformatics*, 15, 717–736, <https://doi.org/10.2166/hydro.2013.132>, 2013.
- Huang, M., Gallichand, J., Dong, C., Wang, Z., and Shao, M.: Use of soil moisture data and curve number method for
565 estimating runoff in the Loess Plateau of China, *Hydrol. Process.*, 21, 1471–1481, <https://doi.org/10.1002/hyp.6312>, 2007.
- Hungerford, H., Smiley, S., Blair, T., Beutler, S., Bowers, N., and Cadet, E.: Coping with Floods in Pikine, Senegal: An Exploration of Household Impacts and Prevention Efforts, *Urban Sci.*, 3, 54, <https://doi.org/10.3390/urbansci3020054>, 2019.
- Kelleners, T. J., Robinson, D. A., Shouse, P. J., Ayars, J. E., and Skaggs, T. H.: Frequency dependence of the complex
570 permittivity and its impact on dielectric sensor calibration in soils, *Soil Sci. Soc. Am. J.*, 69, 67–76, 2005.
- Klutse, N. A. B., Quagraine, K. A., Nkrumah, F., Quagraine, K. T., Berkoh-Oforiwaa, R., Dzrobi, J. F., and Sylla, M. B.: The Climatic Analysis of Summer Monsoon Extreme Precipitation Events over West Africa in CMIP6 Simulations, *Earth Syst. Environ.*, 5, 25–41, <https://doi.org/10.1007/s41748-021-00203-y>, 2021.
- Kreibich, H., Di Baldassarre, G., Vorogushyn, S., Aerts, J. C. J. H., Apel, H., Aronica, G. T., Arnbjerg-Nielsen, K., Bouwer,
575 L. M., Bubeck, P., Caloiero, T., Chinh, D. T., Cortès, M., Gain, A. K., Giampá, V., Kuhlicke, C., Kundzewicz, Z. W., Llasat, M. C., Mård, J., Matczak, P., Mazzoleni, M., Molinari, D., Dung, N. V., Petrucci, O., Schröter, K., Slager, K., Thieken, A. H., Ward, P. J., and Merz, B.: Adaptation to flood risk: Results of international paired flood event studies, *Earths Future*, 5, 953–965, <https://doi.org/10.1002/2017EF000606>, 2017.
- Le Bourgeois, O., Bouvier, C., Brunet, P., and Ayral, P.-A.: Inverse modeling of soil water content to estimate the hydraulic
580 properties of a shallow soil and the associated weathered bedrock, *J. Hydrol.*, 541, 116–126, <https://doi.org/10.1016/j.jhydrol.2016.01.067>, 2016.
- Lericollais, A. and Roquet, D.: Croissance de la population et dynamique du peuplement au Sénégal depuis l’indépendance, *Espace Popul. Sociétés*, 17, 93–106, <https://doi.org/10.3406/espos.1999.1872>, 1999.
- Li, G., Zhao, H., Liu, C., Wang, J., and Yang, F.: City Flood Disaster Scenario Simulation Based on 1D–2D Coupled Rain–
585 Flood Model, *Water*, 14, 3548, <https://doi.org/10.3390/w14213548>, 2022.

- Maref, N. and Seddini, A.: Modeling of flood generation in semi-arid catchment using a spatially distributed model: case of study Wadi Mekerra catchment (Northwest Algeria), *Arab. J. Geosci.*, 11, 116, <https://doi.org/10.1007/s12517-018-3461-2>, 2018.
- Mark, O., Weesakul, S., Apirumanekul, C., Aroonnet, S., and Djordjevic, S.: Potential and limitations of 1D modelling of urban flooding, *J. Hydrol.*, 299, 284–299, [https://doi.org/10.1016/S0022-1694\(04\)00373-7](https://doi.org/10.1016/S0022-1694(04)00373-7), 2004.
- 590 Martínez, C., Sanchez, A., Toloh, B., and Vojinovic, Z.: Multi-objective Evaluation of Urban Drainage Networks Using a 1D/2D Flood Inundation Model, *Water Resour. Manag.*, 32, 4329–4343, <https://doi.org/10.1007/s11269-018-2054-x>, 2018.
- Mashi, S. A., Inkani, A. I., Obaro, O., and Asanarimam, A. S.: Community perception, response and adaptation strategies towards flood risk in a traditional African city, *Nat. Hazards*, 103, 1727–1759, <https://doi.org/10.1007/s11069-020-04052-2>, 2020.
- 595 Meng, X., Zhang, M., Wen, J., Du, S., Xu, H., Wang, L., and Yang, Y.: A Simple GIS-Based Model for Urban Rainstorm Inundation Simulation, *Sustainability*, 11, 2830, <https://doi.org/10.3390/su11102830>, 2019.
- Miller, J., Vischel, T., Fowe, T., Panthou, G., Wilcox, C., Taylor, C. M., Visman, E., Coulibaly, G., Gonzalez, P., Body, R., Vesuviano, G., Bouvier, C., Chahinian, N., and Cazenave, F.: A modelling-chain linking climate science and decision-makers for future urban flood management in West Africa, *Reg. Environ. Change*, 22, 93, <https://doi.org/10.1007/s10113-022-01943-x>, 2022a.
- 600 Miller, J., Taylor, C., Guichard, F., Peyrillé, P., Vischel, T., Fowe, T., Panthou, G., Visman, E., Bologo, M., Traore, K., Coulibaly, G., Chapelon, N., Beucher, F., Rowell, D. P., and Parker, D. J.: High-impact weather and urban flooding in the West African Sahel – A multidisciplinary case study of the 2009 event in Ouagadougou, *Weather Clim. Extrem.*, 36, 100462, <https://doi.org/10.1016/j.wace.2022.100462>, 2022b.
- 605 Mosavi, A., Ozturk, P., and Chau, K.: Flood Prediction Using Machine Learning Models: Literature Review, *Water*, 10, 1536, <https://doi.org/10.3390/w10111536>, 2018.
- Moulds, S., Buytaert, W., Templeton, M. R., and Kanu, I.: Modeling the Impacts of Urban Flood Risk Management on Social Inequality, *Water Resour. Res.*, 57, e2020WR029024, <https://doi.org/10.1029/2020WR029024>, 2021.
- 610 Ndiaye, I.: Étalement urbain et différenciation sociospatiale à Dakar (Sénégal), *Cah. Géographie Qué.*, 59, 47–69, <https://doi.org/10.7202/1034348ar>, 2015.
- Nicholson, S. E., Some, B., and Kone, B.: An Analysis of Recent Rainfall Conditions in West Africa, Including the Rainy Seasons of the 1997 El Niño and the 1998 La Niña Years, *J. Clim.*, 13, 2628–2640, [https://doi.org/10.1175/1520-0442\(2000\)013<2628:AAORRC>2.0.CO;2](https://doi.org/10.1175/1520-0442(2000)013<2628:AAORRC>2.0.CO;2), 2000.
- 615 Nkrumah, F., Vischel, T., Panthou, G., Klutse, N. A. B., Adukpo, D. C., and Diedhiou, A.: Recent Trends in the Daily Rainfall Regime in Southern West Africa, *Atmosphere*, 10, 741, <https://doi.org/10.3390/atmos10120741>, 2019.
- Nkwunonwo, U. C., Whitworth, M., and Baily, B.: A review of the current status of flood modelling for urban flood risk management in the developing countries, *Sci. Afr.*, 7, e00269, <https://doi.org/10.1016/j.sciaf.2020.e00269>, 2020.

- 620 Nouaceur, Z.: La reprise des pluies et la recrudescence des inondations en Afrique de l'Ouest sahélienne, *Physio-Géo Géographie Phys. Environ.*, 89–109, <https://doi.org/10.4000/physio-geo.10966>, 2020.
- Panthou, G., Lebel, T., Vischel, T., Quantin, G., Sane, Y., Ba, A., Ndiaye, O., Diongue-Niang, A., and Diopkane, M.: Rainfall intensification in tropical semi-arid regions: the Sahelian case, *Environ. Res. Lett.*, 13, 064013, <https://doi.org/10.1088/1748-9326/aac334>, 2018.
- 625 Parvin, F., Ali, S. A., Calka, B., Bielecka, E., Linh, N. T. T., and Pham, Q. B.: Urban flood vulnerability assessment in a densely urbanized city using multi-factor analysis and machine learning algorithms, *Theor. Appl. Climatol.*, 149, 639–659, <https://doi.org/10.1007/s00704-022-04068-7>, 2022.
- Pla, G., Crippa, J., Djerboua, A., Dobricean, O., Dongar, F., Eugene, A., and Raymond, M.: ESPADA : un outil pour la gestion en temps réel des crues éclairs urbaines en pleine modernisation, *Houille Blanche*, 105, 57–66, 630 <https://doi.org/10.1051/lhb/2019027>, 2019.
- Ponce, V. M. and Hawkins, R. H.: Runoff curve number: Has it reached maturity?, *J. Hydrol. Eng.*, 1, 11–19, [https://doi.org/10.1061/\(ASCE\)1084-0699\(1996\)1:1\(11\)](https://doi.org/10.1061/(ASCE)1084-0699(1996)1:1(11)), 1996.
- Pons, F., Delgado, J., Guéro, P., Berthier, E., and Ile-de-France, C.: Exzeco: a gis and dem based method for predetermination of flood risk related to direct runoff and flash floods, 9th Int. Conf. Hydroinformatics HIC 2010 Tianjin CHINA, 2063–2070, 2010. 635
- Rabori, A. M. and Ghazavi, R.: Urban Flood Estimation and Evaluation of the Performance of an Urban Drainage System in a Semi-Arid Urban Area Using SWMM, *Water Environ. Res.*, 90, 2075–2082, <https://doi.org/10.2175/106143017X15131012188213>, 2018.
- Rosenzweig, B. R., Herreros Cantis, P., Kim, Y., Cohn, A., Grove, K., Brock, J., Yesuf, J., Mistry, P., Welty, C., 640 McPhearson, T., Sauer, J., and Chang, H.: The Value of Urban Flood Modeling, *Earths Future*, 9, e2020EF001739, <https://doi.org/10.1029/2020EF001739>, 2021.
- Rubinato, M., Shucksmith, J., Saul, A. J., and Shepherd, W.: Comparison between InfoWorks hydraulic results and a physical model of an urban drainage system, *Water Sci. Technol.*, 68, 372–379, 2013.
- Sakijege, T. and Dakyaga, F.: Going beyond generalisation: perspective on the persistence of urban floods in Dar es Salaam, 645 *Nat. Hazards*, 115, 1909–1926, <https://doi.org/10.1007/s11069-022-05645-9>, 2023.
- Sambe-Ba, B., Espié, E., Faye, M. E., Timbiné, L. G., Sembene, M., and Gassama-Sow, A.: Community-acquired diarrhea among children and adults in urban settings in Senegal: clinical, epidemiological and microbiological aspects, *BMC Infect. Dis.*, 13, 580, <https://doi.org/10.1186/1471-2334-13-580>, 2013.
- Sané, O., Gaye, A. T., Diakhate, M., and Aziadekey, M.: Critical Factors of Vulnerability That Enable Medina Gounass 650 (Dakar/Senegal) to Adapt against Seasonal Flood Events, *J. Geogr. Inf. Syst.*, 08, 457–469, <https://doi.org/10.4236/jgis.2016.84038>, 2016.

- Sane, Y., Panthou, G., Bodian, A., Vischel, T., Lebel, T., Dacosta, H., Quantin, G., Wilcox, C., Ndiaye, O., Diongue-Niang, A., and Diop Kane, M.: Intensity–duration–frequency (IDF) rainfall curves in Senegal, *Nat. Hazards Earth Syst. Sci.*, 18, 1849–1866, <https://doi.org/10.5194/nhess-18-1849-2018>, 2018.
- 655 Sène, A., Sarr, M. A., Kane, A., and Diallo, M.: L’assèchement des lacs littoraux de la grande côte du Sénégal: Mythe ou réalité? Cas des lacs Thiourour, Warouwaye et Wouye de la banlieue de Dakar, *J Anim Plant Sci*, 35, 5623–5638, 2018.
- Sène, A. M.: L’urbanisation de l’Afrique: davantage de bidonvilles ou des villes intelligentes ?, *Popul. Avenir*, 739, 14–16, <https://doi.org/10.3917/popav.739.0014>, 2018.
- Sene, S. and Ozer, P.: Evolution pluviométrique et relation inondations – événements pluvieux au Sénégal, *Bull. Société*
660 *Géographique Liège*, 42, 2002.
- Sidek, L. M., Jaafar, A. S., Majid, W. H. A. W. A., Basri, H., Marufuzzaman, M., Fared, M. M., and Moon, W. C.: High-resolution hydrological-hydraulic modeling of urban floods using InfoWorks ICM, *Sustainability*, 13, 10259, 2021.
- Šimůnek, J., Genuchten, M. Th., and Šejna, M.: Recent Developments and Applications of the HYDRUS Computer Software Packages, *Vadose Zone J.*, 15, 1–25, <https://doi.org/10.2136/vzj2016.04.0033>, 2016.
- 665 Skrede, T. I., Muthanna, T. M., and Alfredesen, K.: Applicability of urban streets as temporary open floodways, *Hydrol. Res.*, 51, 621–634, <https://doi.org/10.2166/nh.2020.067>, 2020.
- Steenhuis, T. S., Winchell, M., Rossing, J., Zollweg, J. A., and Walter, M. F.: SCS Runoff Equation Revisited for Variable-Source Runoff Areas, *J. Irrig. Drain. Eng.*, 121, 234–238, [https://doi.org/10.1061/\(ASCE\)0733-9437\(1995\)121:3\(234\)](https://doi.org/10.1061/(ASCE)0733-9437(1995)121:3(234)), 1995.
- 670 Sy, B., Frischknecht, C., Dao, H., Consuegra, D., and Giuliani, G.: Reconstituting past flood events: the contribution of citizen science, *Hydrol. Earth Syst. Sci.*, 24, 61–74, <https://doi.org/10.5194/hess-24-61-2020>, 2020.
- Tadesse, A. and Anagnostou, E. N.: African convective system characteristics determined through tracking analysis, *Atmospheric Research*, 98, 468–477, <https://doi.org/10.1016/j.atmosres.2010.08.012>, 2010.
- Taromideh, F., Fazloulou, R., Choubin, B., Emadi, A., and Berndtsson, R.: Urban Flood-Risk Assessment: Integration of
675 *Decision-Making and Machine Learning*, *Sustainability*, 14, 4483, <https://doi.org/10.3390/su14084483>, 2022.
- Taylor, C. M., Belušić, D., Guichard, F., Parker, D. J., Vischel, T., Bock, O., Harris, P. P., Janicot, S., Klein, C., and Panthou, G.: Frequency of extreme Sahelian storms tripled since 1982 in satellite observations, *Nature*, 544, 475–478, <https://doi.org/10.1038/nature22069>, 2017.
- Tazen, F., Diarra, A., Kabore, R. F. W., Ibrahim, B., Bologo/Traoré, M., Traoré, K., and Karambiri, H.: Trends in flood
680 *events and their relationship to extreme rainfall in an urban area of Sahelian West Africa: The case study of Ouagadougou, Burkina Faso*, *J. Flood Risk Manag.*, 12, e12507, <https://doi.org/10.1111/jfr3.12507>, 2018.
- Tramblay, Y., Bouvier, C., Ayrat, P.-A., and Marchandise, A.: Impact of rainfall spatial distribution on rainfall-runoff modelling efficiency and initial soil moisture conditions estimation, *Nat. Hazards Earth Syst. Sci.*, 11, 157–170, <https://doi.org/10.5194/nhess-11-157-2011>, 2011.

- 685 Williams, D. S., Máñez Costa, M., Sutherland, C., Celliers, L., and Scheffran, J.: Vulnerability of informal settlements in the context of rapid urbanization and climate change, *Environ. Urban.*, 31, 157–176, <https://doi.org/10.1177/0956247818819694>, 2019.
- Yengoh, G. T., Fogwe, Z. N., and Armah, F. A.: Floods in the Douala metropolis, Cameroon: attribution to changes in rainfall characteristics or planning failures?, *J. Environ. Plan. Manag.*, 60, 204–230, <https://doi.org/10.1080/09640568.2016.1149048>, 2017.
- 690 Yuan, Y., Chen, S. S., and Miao, Y.: Unmanaged Urban Growth in Dar es Salaam: The Spatiotemporal Pattern and Influencing Factors, *Sustainability*, 15, 10575, <https://doi.org/10.3390/su151310575>, 2023.
- Zanchetta, A. and Coulibaly, P.: Recent Advances in Real-Time Pluvial Flash Flood Forecasting, *Water*, 12, 570, <https://doi.org/10.3390/w12020570>, 2020.
- 695 Zhang, C., Huang, H., and Li, Y.: Analysis of water accumulation in urban street based on DEM generated from LiDAR data, *DESALINATION WATER Treat.*, 119, 253–261, <https://doi.org/10.5004/dwt.2018.22049>, 2018.
- Zheng, X., Maidment, D. R., Tarboton, D. G., Liu, Y. Y., and Passalacqua, P.: GeoFlood: Large-Scale Flood Inundation Mapping Based on High-Resolution Terrain Analysis, *Water Resour. Res.*, 54, <https://doi.org/10.1029/2018WR023457>, 2018.
- 700 Zhenyu, X. and Olivier, B.: Conception des réseaux d’assainissement: Pluies de projet et norme NF EN 752-2, *Rev. Eur. Génie Civ.*, 9, 401–413, <https://doi.org/10.1080/17747120.2005.9692762>, 2005.
- Zhu, Z., Chen, Z., Chen, X., and He, P.: Approach for evaluating inundation risks in urban drainage systems, *Sci. Total Environ.*, 553, 1–12, <https://doi.org/10.1016/j.scitotenv.2016.02.025>, 2016.

705